Available online at www.sciencedirect.com

ScienceDirect

Energy Procedia 4 (2011) 4379–4386

Energy Procedia

www.elsevier.com/locate/procedia

GHGT-10

Influence of CO_2 on rock physics properties in typical reservoir rock: A CO_2 flooding experiment of brine saturated sandstone in a CT-scanner

Binyam L. Alemu[a,*], Eyvind Aker[b], Magnus Soldal[b], Øistein Johnsen[b] and Per Aagaard[a]

[a]*University of Oslo, P.O.Box 1047 Blindern, N-0312 Olso, Norway*
[b]*Norges Geotekniske Institutt, Sognsveien 72, 0806 Oslo, Norway*

Abstract

Laboratory core flooding experiment was run to investigate the joint use of electrical resistivity, ultrasonic velocities and 3D images of fluid distribution to improve current understanding of CO_2 and brine behaviour during drainage and imbibition in reservoir rocks. The test specimen was cylindrical Rothbach sandstone measuring 100 mm in length and 38 mm in diameter, with a porosity of 23% and an average permeability of 400 mD. The brine saturated specimen was drained by injecting CO_2 and later imbibed with brine while monitoring changes in resistivity and ultrasonic velocity measurements. Actual fluid saturation level and distribution have been mapped simultaneously using X-ray CT scan. CO_2 saturation calculations based on CT values showed a steep saturation gradient at start of drainage and the gradient flattened with more CO_2 injected into the sample. The ultrasonic compressional velocity (V_p) measurements depicted a continuous decrease with increase in CO_2 saturation while the resistivity of the sample increased proportionally with increase in CO_2 saturation. A CO_2 saturation of 53% was achieved at the end of drainage after injection of 20 pore volume (PV) CO_2. This resulted in a decrease of V_p by 7.2% while the amplitude decreased by as much as 48%. At the end of drainage, the resistivity of the sample increased to 13.9 Ω-m from full brine saturated value of 3.2 Ω-m. During imbibition, the sample was re-saturated close to 100% after 10 PV brine injection. Change in V_p due to CO_2 saturation level variation was relatively consistent during drainage and imbibition (no hysteresis) where as the resistivity of the sample was more affected by the flooding history resulting in hysteretic variation in resistivity. Resistivity index (RI) values did not show a consistent pattern and a single Archie's saturation exponent (n) could not be assigned.

Key words: CO_2; drainage; imbibition; resistivity index; ultrasonic velocity; saturation

1. Introduction

In recent years, underground storage of carbon dioxide (CO_2) from large scale point sources have been considered as one of the main options for reducing anthropogenic CO_2 emissions. The success of such techniques is highly dependant on the capacity of these repositories to be able to store CO_2 with no significant leakage back to the atmosphere. Since much of the CO_2 stored will initially be trapped hydro-dynamically, a clear understanding of the

* Corresponding author. Tel.: +47 228 54 908; fax: +47 228 54 215.
E-mail address: b.l.alemu@geo.uio.no

doi:10.1016/j.egypro.2011.02.390

basic mechanisms of transport through the reservoir, as well as measurement and outlining of CO_2 plume is vital for quantification, monitoring and detecting of potential CO_2 leakage during and after injection. Indirect geophysical measurements have been employed to detect and measure the distribution of CO_2 plume in geological storage sites [eg. 1]. However they are highly dependent on the relative saturation and distribution of the specific fluids (e.g. brine and CO_2) in the pore space. Simultaneous use of both electrical resistivity and seismic velocity measurements enable two complementary measurements. Seismic velocity measurements have better resolution efficiency in fluid mapping in geological reservoirs compared to electrical resistivity where as the latter has better precision in terms of quantifying relative saturation levels of immiscible fluids. In the presented work, saturation levels and distribution of fluids within the porous system is mapped in real time using high resolution X-ray Computed Tomography (CT) scanner. This gives additional information compared to ordinary imbibition and drainage experiments since saturation levels are not averaged from amounts of fluid injected and produced, but from actual fluid distribution and saturation levels obtained from CT images. Hence, the effect of fluid distribution within the sample on the measured geophysical properties can be investigated. The laboratory experiment was conducted with the purpose of better understanding fluid distribution in a reservoir rock and for determining the potential to estimate saturation level of CO_2 in geological reservoirs using seismic and electromagnetic surveys.

2. Material and methods

2.1. Experimental setup

A new experimental setup (Figure 1) has been designed using a specially built core holder that is made of a composite structure of steel and carbon-fiber. The central part of the cell, where the rock core is placed, is made from pure carbon-fiber which is highly transparent to X-ray. The facility allows continuous injection of fluids into the sample at room temperature. The top and bottom cap of the cell are electrically separated such that electrical resistivity across the sample can be measured. The pumps connected to the top cap are electrically separated from the rest of the system to avoid current leakage during the test. Electrical measurements were made using the top and bottom pedestals as electrodes while 1 kHz and 4V excitation is sent through the bottom pedestal. Thus, the potential difference between top and bottom pedestals is used to calculate the resistivity of the core at given fluid saturation. Piezoceramic crystals in the top and bottom pedestals were used for measurement of compressional and shear ultrasonic velocities at a frequency of 500 kHz. Details of the simultaneous use of velocity and resistivity measurements are given in [2]. The system is equipped with a logging facility where pore pressure, temperature, flow rate and volume are continuously recorded. A two-head Isco™ syringe pump was used to keep a constant pore pressure during injection, while GDS™ pumps were used to control injection rate and volume. The set up is configured in such a way that the Isco pumps are set to keep a constant pressure of 10 MPa while the GDS is taking fluids into the pump at a given rate and required volume. The cell pressure (i.e. the confining pressure) was maintained by GDS pump at 25MPa. Pressure transducer was mounted close to the cell to monitor change in pore pressure. The entire setup is built outside the CT-scanner cabinet and logging cable and pipe lines are connected after the cell is mounted inside the CT- scanner. Each scan takes approximately 1 hour. Unlike medical CT-scanner, the entire cell is rotated with fixed X-ray source and detector. The piping and the logging cables are specially setup to allow 360 º rotations at experimental pressure.

2.2. Experimental procedure

The test specimen is a cylindrical Rothbach sandstone sample measuring 100 mm in length and 38 mm in diameter, with an average porosity of 23 % and an average permeability of 400 mD. The sample has a heterogeneous structure and it was drilled perpendicular to the layering. It is mainly composed of quartz, feldspar and small percentage of clay. Synthetic brine with 50g/l total solids (40 g/ NaCl and 10g/L NaI) and resistivity of 0.16 Ω-m was used in the experiment. NaI was added to the solution as a dopant to increase contrast between CO_2 and brine during X-ray CT-scan. The core holder with a dry sample was mounted in the CT- scanner and CT- images of dry, CO_2 saturated, and brine saturated sample were collected sequentially. Both electrical resistivity and ultrasonic measurements were taken at the above three saturation conditions. The CO_2 was allowed to equilibrate inside the pump at room temperature and experimental pressure conditions before injection started. During the test liquid CO_2 (at 20°C and 10MPa) is injected into a brine saturated sandstone core that is kept at isotropic confining pressure of 25 MPa. The

CO_2 is injected stepwise while measuring electrical resistivity, ultrasonic velocities and simultaneously scanning the rock by X-ray CT scans. To study the effect of imbibition of brine and subsequent dissolution of CO_2 into brine, a similar procedure was used to imbibe the core with brine after the initial CO_2 flooding until the sample was re-saturated to a level close to 100% brine saturation. Fluids were injected into the core at 0.2 pore volume (PV= 26.1 mL), per each step and at a rate of 0.3mL/min until 2 PV has been pumped. An injection rate of 0.5, 1.0 and 5 mL/min were used for volume pumped between 2-6, 6-10 and 10-20 PV, respectively. The injection steps used for the experiment were (0.1, 0.3, 0.5, 0.7, 0.9, 1, 2, 6, 10, 13, and 20 PV) for drainage and 0.1, 0.3, 0.5, 0.7, 0.9, 1, 2, 4, 6, and 10 PV) for imbibition. Values are cumulative injected fluid volume at each step.

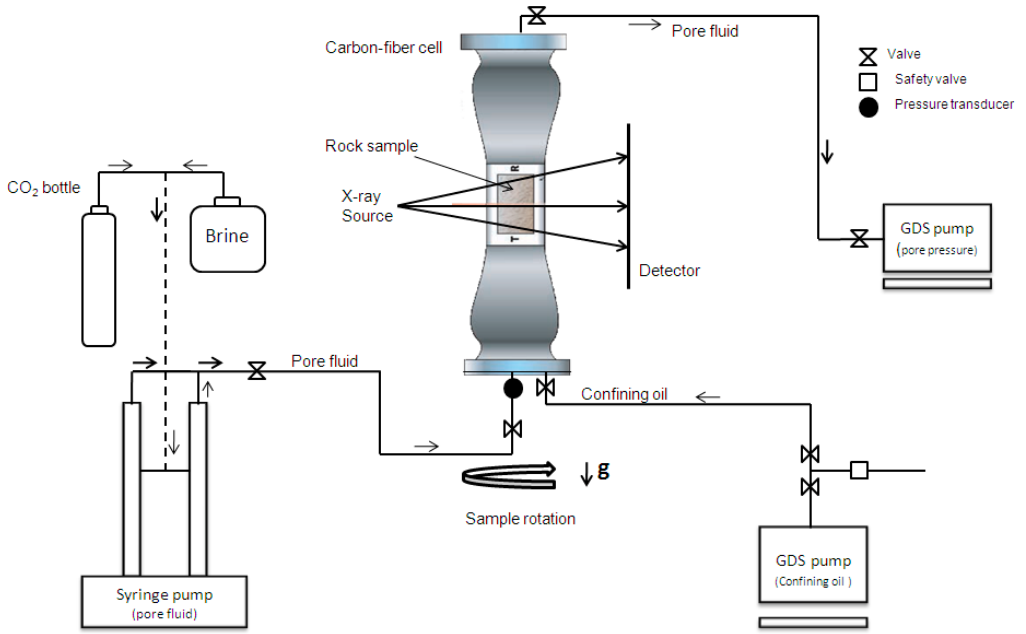

Figure 1: Schematic diagram of experimental setup at NGI laboratory used for the experiment. T and R inside the core holder stand for transmitter and receiver. Picture of the sample holder is modified from [3].

The X-ray CT pictures were collected 1 hour after the injection of fluid was completed to allow the system to stabilize following initial dissolution of CO_2 in the brine. The time limit was chosen based on trial test runs prior to the start of the experiment. Each scan takes 1 hour and the time between two successive injections was 2 hours. During the first hour, both velocity and resistivity measurements were taken to detect geophysical variations due to dissolution and redistribution of fluids in the pore systems. All the CT images were collected at X-ray configuration of 100 kV, 200uA. The output CT image is digitized as a TIFF-formatted 16-bit image file (2000 x 2000 pixels). Stacks of 2D projection images created during the CT-scan (1000 still pictures/360º rotation) are used to reconstruct 3D volume images. Each voxel in the volume is then assigned a gray value (CT number) that is proportional to the X-ray attenuation property of the material. X-ray attenuation is a function of density, experimental condition (pressure and temperature) and chemical composition of the material in each voxel. CT numbers for pore fluids (air, brine and CO_2) were measured at experimental X-ray configuration by injecting fluid in cylindrical hole drilled in similar sandstone that is mounted in the core holder. Using 3D volume images and measured fluid CT values, porosity (φ) and CO_2 saturation(S_{CO2}) in the sample were calculated using Eq. 1 and 2 [4].

$$\varphi = \frac{CT_{brine,\,r} - CT_{dry,\,r}}{CT_{brine} - CT_{air}} \quad (1)$$

$$S_{CO_2} = \frac{CT_{exp,r} - CT_{brine,r}}{CT_{CO2,r} - CT_{brine,r}} \quad (2)$$

$$S_{brine} = 1 - S_{CO_2} \quad (3)$$

where, $CT_{dry,r}$, $CT_{brine,r}$ and $CT_{CO2,r}$ are CT values of dry, brine, CO_2 saturated rock respectively. $CT_{exp,r}$ is the CT value of the rock at each injection step and CT_{air} and CT_{brine} are CT number of the fluids air and brine.

3. Results

Fluid saturation levels and distribution patterns in the sample were mapped by CT-scanner while electrical resistivity and ultrasonic velocity measurements were taken simultaneously. The top and bottom 10 mm of the sample has been excluded from the image analysis as the interference from the steel pedestals created shadows due to the high X-ray attenuation of steel. Therefore the results presented here; porosity and saturation calculations are representative of the middle 80mm section. Injection of CO_2 at 20 ºC and 10MPa into a brine saturated sample brought major changes in the geophysical properties of the sample resulting a reduction in amplitude and V_p as well as a remarkable increase in electrical resistivity. Since the sample was drilled perpendicular to layering alternating layers of low and high porosity can be seen on the porosity profile (Figure 2). The porosity was low in the middle part of the sample compared to the other regions of the sample. During drainage, brine was not efficiently removed from these low porosity regions.

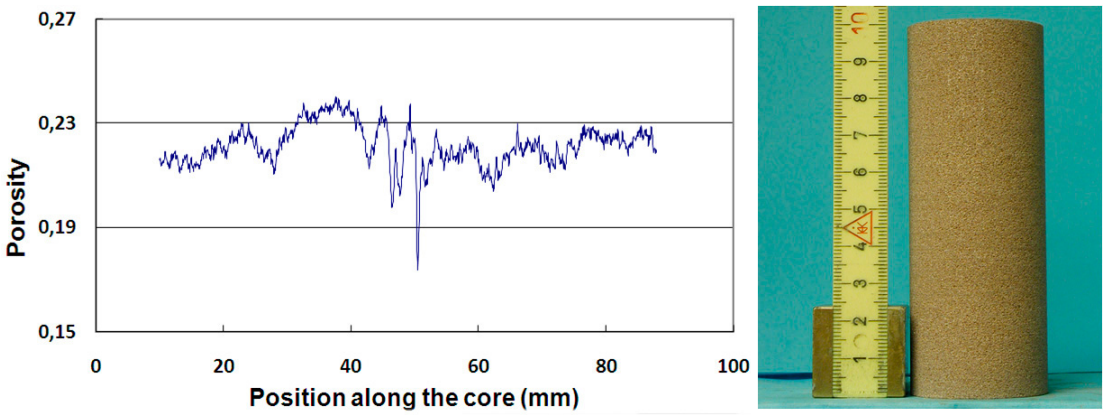

Figure 2: Profile of mean porosity across the length of the core (10-90 mm) left and picture of core used in the experiment, right. Porosity is calculated from CT images using Eq. 1.

The saturation profiles indicate steep gradient for the first few pore volumes (<1 PV) of CO_2 injected (Figure 3). Breakthrough of CO_2 occurred after injection of only 0.5 PV CO_2. As more CO_2 is injected the fluid saturation along the sample became relatively uniform. Both geophysical measurements were taken across the length of the sample and hence are very much influenced by the variation in fluid saturation in the core. The final residual water saturation after 20 PV CO_2 injection was 47 %. This indicates low replacement efficiency by CO_2 compared to that of brine where 10 PV injection of brine into the sample resulted in a re-saturation of the core close to 100 %. In the low porosity layers, brine was not efficiently drained by the CO_2 as it opted to follow highly permeable pathways (larger pore sizes) during drainage. This is clearly seen at lower CO_2 saturations (the first three saturation profile images in Figure 3B), where layers of low porosity regions tend to have very high brine saturation. Hence, sample heterogeneity plays an important role in the distribution of fluids within the core during flooding experiments.

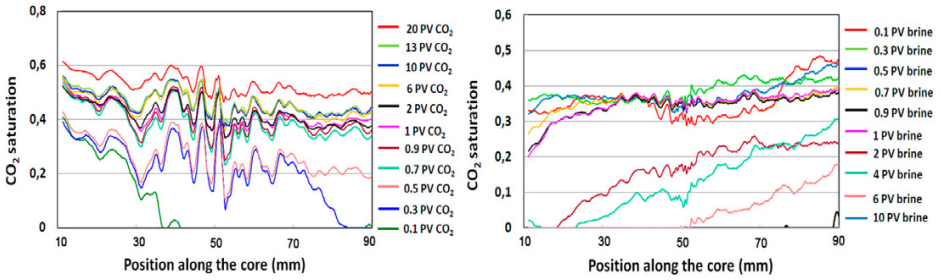

Figure 3A: Average CO_2 saturation along the length of the core, drainage (left) and imbibitions (right). Saturation levels are calculated from CT images using Eq. 2.

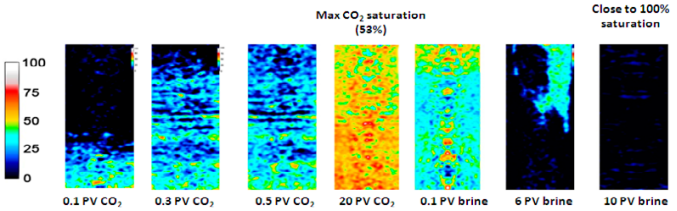

Figure 3B: CO_2 saturation (section images not to scale) along the length of the core of drainage (left) and imbibitions (right). Saturation levels are calculated from CT images using Eq. 2. Images depicted are made by averaging 15pixel radius and bottom and top 1cm of the sample are not indicated due to interference from top and bottom caps.

The compressional velocity (V_p) decreased significantly after injection of 1 PV CO_2 and does not seem to be affected significantly with additional injection of CO_2 beyond 2 PV (Figure 4A). The V_p measured at maximum CO_2 saturation of 53% is 7.2% lower than brine saturated velocity and only 4% higher than the value measured at 100% CO_2 saturation (Figure 5). The change in amplitude did not show a proportional decrease with increase in injected CO_2 volume. However, the amplitude fell sharply after injection of 0.3PV and remained relatively unchanged before it increased after injection of 1 PV CO_2 and remained more or less the same. The variation in amplitude might have been affected by the fluid distribution in the sample as the existence of sharp front (impedance contrast) within the core resulted in a much higher fall in amplitude (attenuation) at lower saturations compared to values measured at higher CO_2 saturation (Figure 4B). Over all, the amplitude fell by 48% after 20PV of CO_2 was injected. Compared to the change in V_p, the change in amplitude due the fluid substitution is much higher. This indicates that amplitude has an advantage over velocity measurements to detect CO_2 in the sandstone especially in outlining CO_2-brine contact. However, both parameters are only sensitive within a narrow window of CO_2 saturation (0-30%) as depicted in Figure 4 A and B.

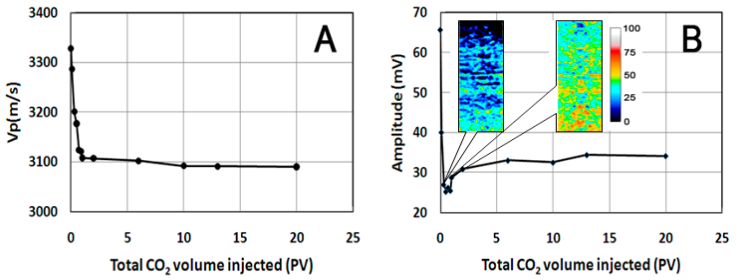

Figure 4: A) Plot of changes ultrasonic compressional velocity, B) amplitude against injected volume of CO_2 during drainage. Section images indicated in B depict that the presence of sharp impedance contrast (after 0. 3 PV) resulting much higher drop in amplitude compared to amplitudes measured at higher CO_2 saturation and insignificant impedance contrast (e.g., 2 PV CO_2).

Plot of V_p against saturation (Figure 5A) depicts a linearly decreasing velocity as CO_2 saturation increased in the core both during drainage and imbibition. V_p was not very much affected by hysteresis effect as the drainage and imbibition lines follow more or less the same pattern. As expected, the shear wave velocity (V_s) was not sensitive to variation in fluid composition (Figure 5B).

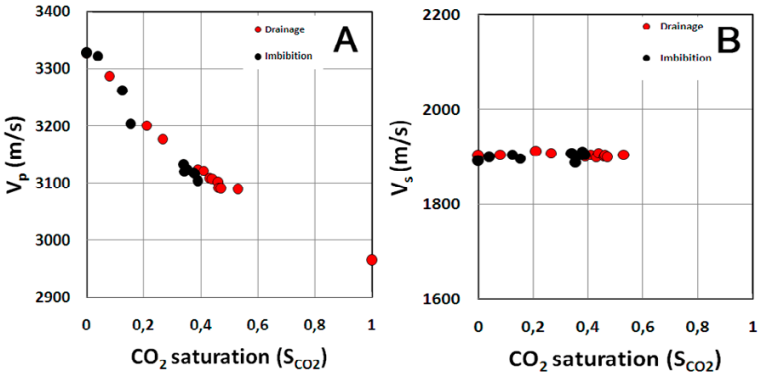

Figure 5: A) Ultrasonic compressional velocity and B) shear velocity variation against average CO_2 saturation in the core.

A method of relating hydrocarbon saturation level in clean sandstone reservoirs with electrical resistivity is described by Archie saturation equation [5].

$$RI = R/R_0 = (S_w)^{-n} \quad (4)$$

Where the resistivity index, RI, is equal to the ratio of the resistivity of the sample (R) at partial brine saturation S_w, over the resistivity of the sample at 100% brine saturation (R_o) and *n* is Archie's saturation exponent. R_o depends on rock effective porosity (φ); a quantity that takes account of the entire system of interconnected pores and excludes isolated voids. R_o can be expresses as:

$$R_0 = R_w F \quad (5)$$

Where R_w is resistivity of brine phase and F formation factor given by:

$$F = a\varphi^{-m} \quad (6)$$

where, *a* is the humble factor and *m* the cementation index. The resistivity of the sample increased to 13.9 from fully brine saturated values of 3.2 Ω-m. After imbibition, the resistivity of the core fell back to fully brine saturated values after injection of 10 PV brine indicating a close to 100% brine saturation. Plot of RI against S_w shown in Figure 6 depicts a non linear trend. However the points are scattered and resistivity values seems to depend more on the flooding history (drainage vs. imbibition) and fluid distribution than what is observed with V_p. Hence, Archie's saturation exponent (n) was not calculated and more analysis and experiments are necessary in order to assess the effect of fluid distribution on the rock resistivity and heterogeneity. This might also have important consequences when deciding location of electrodes in geological storage sites.

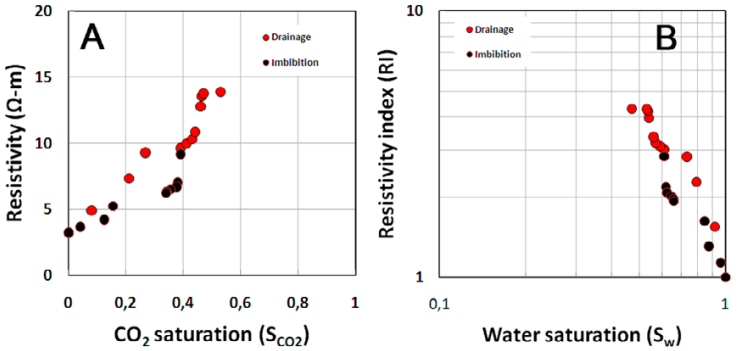

Figure 6: A) Resistivity, B) resistivity index (RI) against calculated average saturation of the core.

At the start of drainage experiment, the resistivity of the core decreased exponentially during the first hour after injection of CO_2. The change in resistivity measured after injection of 0.1PV and 0.3PV CO_2 in to the brine saturated sample has dropped by as much as 9% and 2.5% respectively within 1 hour (Figure 7). As more CO_2 is injected into the core the observed change in measured resistivity with time decreased. The pore pressure in the sample has also decreased during this period on average by 0.2 MPa. However, the same change in resistivity was not observed during imbibition which was constant at all stages. When CO_2 is injected from the bottom into the brine saturated core it occupies the bottom of the sample overlain by a brine saturated column (Figure 7C). Since resistivity is measured along the length of the sample, CO_2 will obstruct the electrical communication in all the pores it occupies. Therefore, any dissolution of CO_2 in these pores will have a high chance of re-establishing the original conduction line since CO_2 column is relatively thin (Figure 7C, 0.1PV CO_2). As the column of CO_2 gets thicker, the potential of re-establishment of a fully brine connected pore decreases even if a fair amount of CO_2 dissolves (Figure 7C, 0.3 PV CO_2). Hence, it causes smaller change in resistivity. During imbibition, injection of brine into the core with a high CO_2 saturation creates a scenario in which a much conductive layer is underlain by a less conductive layer (Figure 7C, 0.1PV brine). Therefore, any re-establishment of electrical conduction by fluid substitution/dissolution at the bottom may not result in change in resistivity unless the electrical conduction is established over the entire length.

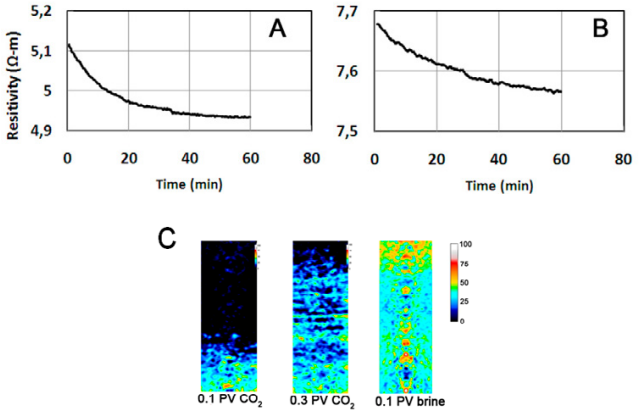

Figure 7: Variation of measured average resistivity of the core along the length of the core in the first hour after end of injection of CO_2. A) 0.1 PV CO_2, B) 0.3 PV CO_2 and C) Saturation cross-section images

Between the end of drainage and beginning of imbibition flooding, the sample was left for 72 hours at the same pressure and temperature conditions. During this time, the resistivity of the sample increased by 6% even if the CO_2 saturation decreased. The decrease in CO_2 saturation of the sample is due to dissolution into the brine phase and a very small diffusion of CO_2 across the rubber membrane and into the hydraulic oil providing an effective confining

pressure of 15 M Pa. The diffusion was confirmed by a separate test where CO_2 was detected in the confining oil where as no leakage of oil into the core was detected. The increase in resistivity is probably related to the accumulation of CO_2 on the top part of the sample that disrupted the electrical conductivity along the core. This can be clearly seen (Figure 7C, 0.1 PV brine) where CO_2 is accumulated at the top part due to buoyancy driven upward migration of CO_2.

Conclusion

Geophysical properties of the sample were affected not only by the level of CO_2 saturation, but also, by the distribution of CO_2 within the sample. After injection of 20 PV CO_2, the saturation of CO_2 in the sample reached 53% and close to 100% brine saturation was achieved by imbibing the sample with 10 PV brine. The absence of significant amount of residual CO_2 might be a result of dissolution CO_2 in the brine. At the end of drainage, V_p and amplitude decreased by 7.2% and 48% respectively, where as, resistivity of the sample increased to 13.9 Ω-m from fully brine saturated value of 3.2 Ω-m. The fact that fluid distribution is mapped using the CT-scanner revealed the dependence of laboratory measured geophysical parameters of rocks in the amount and distribution of fluids in the core. Additional studies are required to understand the full dynamics of CO_2-brine in geological storage reservoirs especially on the dissolution and transport of CO_2 within a similar system.

Acknowledgements

This work is part of the "Subsurface storage of CO_2, Risk Assessment, Monitoring and REmediation" (SSC RAMORE) project. The project is founded by a consortium including The Research Council of Norway, Statoil, RWE Dea, Norske Shell, Conocophillips and Schlumberger. Research performing partners are University of Oslo, University of Bergen, Institute for Energy Research (IFE) and Norwegian Geotechnical Institute. We would like to thank our partners for their financial support.

The authors would also like to thank Gudmund Havstad, Sven Vangbæk, Pawel Jankowski, Ole Petter Rotherud Lloyd Warren Tunbridge and Toralv Berre for their valuable advice and technical support in the design and building of the experimental setup.

References

[1] R. Arts, O. Eiken, A. Chadwick, P. Zweigel, B. van der Meer and G. Kirby. Geological Society, London, Special Publications. 2004; 233: 181-191

[2] Z.Wang, L.J. Gelius, and F.N. Kong. Simultaneous core sample measurements of elastic properties and resistivity at reservoir conditions employing a modified triaxial cell – a feasibility study, Geophysical Prospecting. 2009; 57: 1009-1026.

[3] K. Monsen, and S.E. Johnstad. Improved understanding of velocity–saturation relationships using 4D computer-tomography acoustic measurements. Geophysical Prospecting. 2005; 53: 173-181.

[4] Akin, S. and Kovscek. A. R., Computed tomography in petroleum engineering research. Geological Society London, Special Publications. 2003; 215: 23-38.

[5] D. Zhou, S. Arbabi and E. H. Stenby. A Percolation Study of wettability Effect on the Electrical Properties of Reservior Rocks. Transport in Porous Media. 1997; 29: 85–98.

[6] A. K. Moss, X.D. Jing and J.S. Archer. Journal of Petroleum Science and Engineering. 1999; 24: 231-242.

[7] P. S. Denicol and X. D. Jing. Effects of water salinity, saturation and clay content on the complex resistivity of sandstone samples. Core-Log Integration, Geological Society, London, Special Publications. 1998; 136: 147-157